**Naval Research Laboratory**

Washington, DC 20375-5000

AD-A239 530

NRL Report 9344

# Chemical Reduction of Intermodulation Interference Caused by Metal-Oxide-Metal Junctions Aboard Ship

R. HYNES, H. W. CARHART, AND J. C. COOPER

*Navy Technology Center for Safety and Survivability*
*Chemistry Division*

July 31, 1991

DTIC
ELECTE
AUG 19 1991
S B D

91-08000

Approved for public release; distribution unlimited.

91 8 15 043

# REPORT DOCUMENTATION PAGE

Form Approved
OMB No. 0704-0188

Public reporting burden for this collection of information is estimated to average 1 hour per response, including the time for reviewing instructions, searching existing data sources, gathering and maintaining the data needed, and completing and reviewing the collection of information. Send comments regarding this burden estimate or any other aspect of this collection of information, including suggestions for reducing this burden, to Washington Headquarters Services, Directorate for Information Operations and Reports, 1215 Jefferson Davis Highway, Suite 1204, Arlington, VA 22202-4302, and to the Office of Management and Budget, Paperwork Reduction Project (0704-0188), Washington, DC 20503.

| 1. AGENCY USE ONLY (Leave blank) | 2. REPORT DATE | 3. REPORT TYPE AND DATES COVERED |
|---|---|---|
| | July 31, 1991 | |

**4. TITLE AND SUBTITLE**

Chemical Reduction of Intermodulation Interference Caused by Metal-Oxide-Metal Junctions Aboard Ship

**5. FUNDING NUMBERS**

**6. AUTHOR(S)**

Robert Hynes, Homer W. Carhart, and John C. Cooper

**7. PERFORMING ORGANIZATION NAME(S) AND ADDRESS(ES)**

Naval Research Laboratory
Washington, DC 20375-5000

**8. PERFORMING ORGANIZATION REPORT NUMBER**

NRL Report 9344

**9. SPONSORING/MONITORING AGENCY NAME(S) AND ADDRESS(ES)**

Space and Naval Warfare Systems Command
Washington, DC 20363-5100

**10. SPONSORING/MONITORING AGENCY REPORT NUMBER**

**11. SUPPLEMENTARY NOTES**

**12a. DISTRIBUTION/AVAILABILITY STATEMENT**

Approved for public release; distribution unlimited.

**12b. DISTRIBUTION CODE**

**13. ABSTRACT** (Maximum 200 words)

Intermodulation interference from metal-oxide-metal nonlinear junctions near high frequency transmitters and receivers is suppressed effectively by application of chemical mixtures that provide an alternate, low impedance current path across the junction. The chemical formulations incorporate conductive and high dielectric constant materials into polymers. The mixtures clean metal oxides from surfaces, inhibit further corrosion, and can be used as additives to MILSPEC paints and lubricants. The approach greatly reduces intermodulation interference from electromagnetically active junctions in shipboard applications.

| 14. SUBJECT TERMS | | | 15. NUMBER OF PAGES |
|---|---|---|---|
| Electromagnetic interference | Broadband noise | IMI | 32 |
| Chemical suppression | Intermodulation interference | EMI | 16. PRICE CODE |
| | EMC | BBN | |

| 17. SECURITY CLASSIFICATION OF REPORT | 18. SECURITY CLASSIFICATION OF THIS PAGE | 19. SECURITY CLASSIFICATION OF ABSTRACT | 20. LIMITATION OF ABSTRACT |
|---|---|---|---|
| UNCLASSIFIED | UNCLASSIFIED | UNCLASSIFIED | SAR |

NSN 7540-01-280-5500

Standard Form 298 (Rev 2-89)
Prescribed by ANSI Std 239-18
298-102

## CONTENTS




For
I
d
ion
ion/
lity Codes
l and/or
Special
Dist
A-1

# CHEMICAL REDUCTION OF INTERMODULATION INTERFERENCE CAUSED BY METAL-OXIDE-METAL JUNCTIONS ABOARD SHIP

## INTRODUCTION

This report describes rusty-bolt intermodulation interference (IMI) research and experiments that evaluate the ability of different materials to reduce IMI in metal-oxide-metal (MOM) junctions.[1]

Naval ships and aircraft have many sophisticated emitters and receivers. This makes the nature of the electromagnetic environment (EME) critical. As metallic joints corrode, they sometimes produce semiconductor junctions. When this occurs, they absorb radio frequency (RF) energy from the ships' transmitting antennas and reradiate (IMI) products of the absorbed frequencies. This is commonly called the rusty bolt effect. Even though power reradiated in this way is low relative to shipboard transmitter effective radiated power (ERP), it is still high enough to have a devastating impact on shipboard communications, electronic warfare, and intelligence gathering equipment. This is because:

(1) The number of transmitting antennas and the power radiated by a Naval vessel is very large compared to that of a commercial ship, thereby enhancing the potential IMI effect.

(2) The potential number of electronically active rusty bolts is large.

(3) The potential number of discrete frequencies generated by each rusty bolt is large.

(4) The reradiated power level is large compared to that of the desired received signals. The vessel listens to threat signals with extremely sensitive receivers which can detect energy at very low power levels ( $<10^{-6}$v/m). Even a low level of spurious energy can compete with these

---

[1] Coauthor John C. Cooper died in December 1990. This report is dedicated to his memory and his many insightful contributions to the subject.

Manuscript approved July 2, 1991.

signals and jam sensitive shipboard receivers. The third order IMI level aboard some ships is more than 60 dB above the ships' receivers minimum detectable signal level.

The suppression of IMI products from noisy junctions can be effected in a number of ways. In some cases it may be possible to decouple the junction from its natural antenna minimizing the RF current and, therefore, the generation of IMI products. Alternatively, the junction area may be electrically bypassed with a ground strap. In many instances these methods are not applicable, and chemical treatments are being developed to modify the electrical properties of the junctions. The two basic methods that can be applied are (1) to cause additional corrosion in order to make the junction an open circuit, or (2) to modify the surface oxides in the junction to form a linear, closed circuit path for RF current. Neither of these is easy to accomplish in a controlled fashion, so it is vital to understand the basic chemistry and physics in the interface between the metal to oxide contacts.

This report documents the development of techniques and materials for chemical suppression of electromagnetically active junctions aboard ship and how they were tested in the laboratory and at sea. Also reported is an account of the interfacial electrochemistry of Fe-Oxide-Fe (Fe-O-Fe) junctions resulting in a theoretical model of the current-voltage (I-V) characteristic that has been used to predict the IMI spectral component distribution from the nonlinear junctions by using Fourier Transform analysis. This work has led to a deeper understanding of the criteria responsible for maximizing or minimizing IMI products from nonlinear junctions and to the design of chemical treatments for the suppression of IMI.

## IMI PHYSICS

Rusty bolt IMI occurs when RF signals mix in a nonlinear junction. In a linear junction (ohmic contact), two signals form a simple algebraic sum. In a nonlinear junction, the I-V curve is nonlinear. That is, the current through the junction is not linearly related to the applied voltage. This nonlinearity causes the waveform to be modified as it traverses the junction. The result is a complicated waveform with many harmonics. When more than one frequency is applied to a nonlinear junction, it generates new signal components according to the formula:

$$F_i = m_1 f_1 \pm m_2 f_2 \pm \ldots m_n f_n,$$

where

$m_1, m_2, \ldots m_n$ each take on the values of the set of all positive integers;
$f_1, f_2, \ldots f_n$ are the frequencies of the RF signals; and $F_i$ is the intermodulation frequency,

and where

$$Q = m_1 + m_2 + \ldots m_n = \text{the order of the IMI.}$$

This generates many new frequencies that are sums and differences of integral multiples of all the

applied signals and their harmonics. It is customary in IMI testing to use a pair of frequencies: $f_1$ and $f_2$. Naturally occurring nonlinear junctions usually consist of metallic joints that have corroded due to exposure to weather. As a first step in understanding the nonlinearity of a junction, it is customary to consider the ideal diode whose I-V curve is shown in Fig. 1, as defined by the equation:

$$I_j = I_o[\exp(eV_j/kT) - 1]$$

where

$I_j$ is the junction current,
$I_o$ is the saturation current,
$e$ is the electron charge,
$V_j$ is the junction voltage,
$k$ is the Boltzmann's constant, and
$T$ is the absolute temperature.

The resistance $R$ is essentially the result of the bulk resistance of the p-n junction. Both the heuristic explanation and rigorous mathematical derivation of this curve based on field theory, solid state space charge, Fermi levels, diffusion current, work functions of the materials, depletion regions, and diffusion capacitance are widely available [1 to 5].

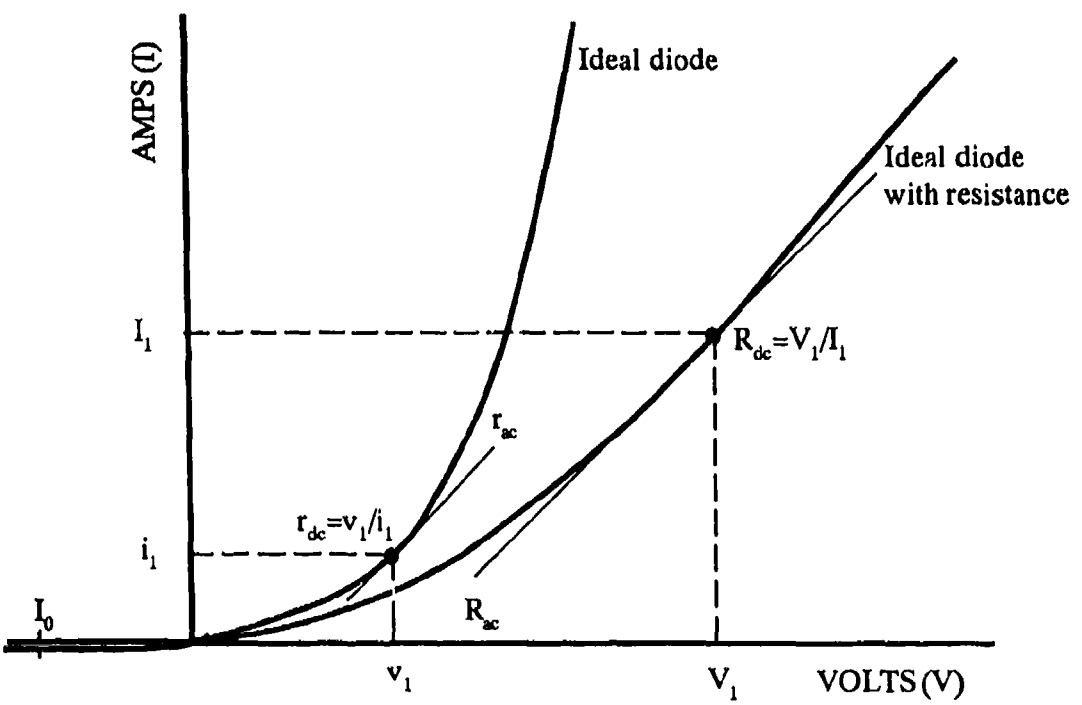


Fig. 1 - The ideal diode

The d-c resistance of the ideal diode $r_{dc}$ can be determined graphically as indicated in Fig. 1 or calculated as

$$r_{dc} = V_j/I_j = V_j/I_o[\exp(eV_j/kT) - 1].$$

Figure 1 shows that the a-c resistance of the ideal diode can be determined graphically as the slope of the I-V curve at the operating point or calculated as the reciprocal of conductance $g_{ac}$:

$$g_{ac} = dI_j/dV_j = (I_o e/kT)\exp(eV_j/kT),$$

and

$$r_{ac} = 1/g_{ac}.$$

In the shipboard case, as indeed with any real diode junction, there is always ohmic resistance in the circuit. Therefore, at high current levels, the ideal-diode resistance becomes negligible with respect to the bulk resistance of the junction, and the curve becomes essentially linear.

The ideal diode equation as illustrated in Fig. 1 shows that for any reverse voltage, however large, the junction current equals the saturation current $I_0$. This does not account for leakage current along the edges of the junction, which is a small effect. Nor does it account for reverse breakdown, which is a major effect in real metal-semiconductor (MS) junctions and which is a key factor in IMI generation aboard ship. Figure 2 shows the reverse breakdown phenomenon.

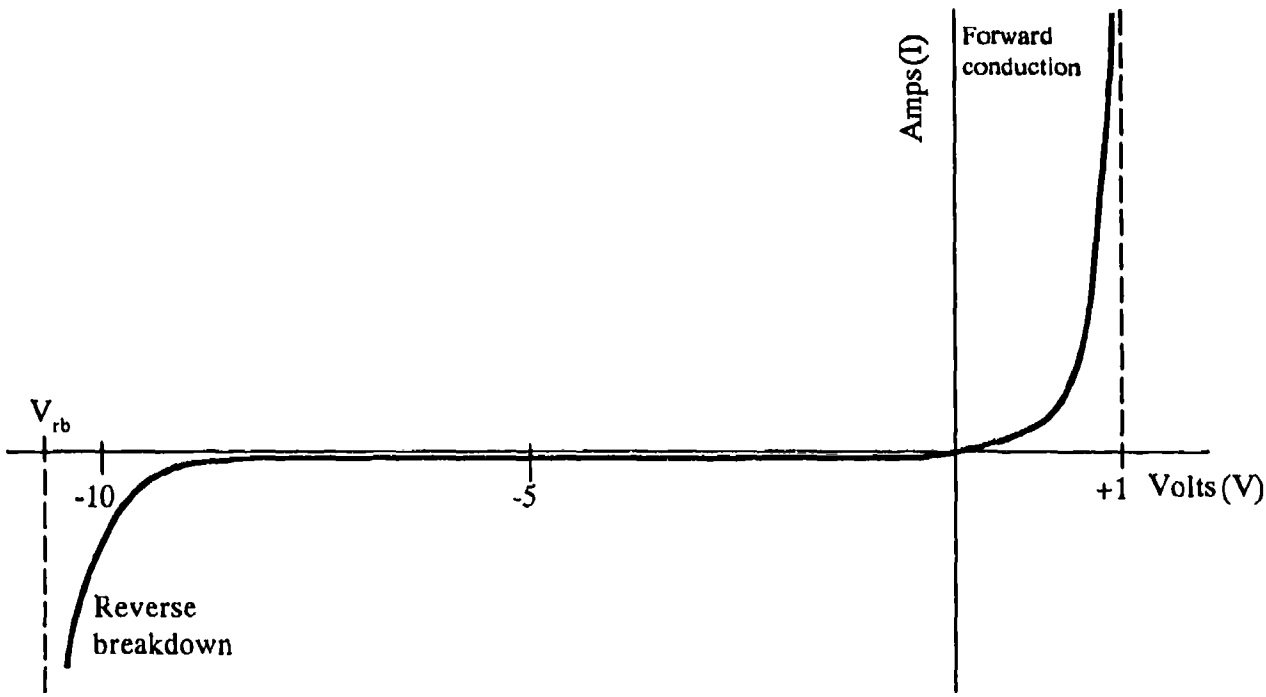


Fig. 2 - Metal semiconductor junction I-V characteristic showing reverse breakdown

There are two mechanisms that cause reverse breakdown in a junction diode: Zener breakdown and avalanche breakdown. Zener breakdown occurs in very narrow junctions (< 200 nm); avalanche breakdown occurs in relatively wide junctions (>1000 nm). These distances apply to silicon and germanium crystals and would have different values for other semiconductors, including several forms of rust. Because of the very narrow physical dimension of the depletion region in an MS junction, an externally applied voltage of a few volts across a junction with a conductivity of 100 mhos/m can cause a potential gradient of $10^6$ V/m across the depletion region, which is sufficient to cause ionization in the junction. Experiments show that in silicon and germanium, junctions that breakdown at 4 V or less do so by Zener breakdown with direct field ionization of electrons from the valence to the conduction band (tunneling) [4]. Junctions that breakdown at 8 V or more do so by secondary ionization (avalanche). Junctions that breakdown between 4 V and 8 V have a mixture of avalanche and tunneling.

Turning away from theoretical considerations of reverse breakdown now, we focus on practical MS junctions in the laboratory and aboard ship. Figure 3 shows the macro-equivalent circuit of an MS junction and its I-V curve. Forward conduction occurs at $V_0$, which typically has a value in the range from 0.5 to 0.7 V, depending on the materials of the junction. Reverse breakdown occurs at $V_{rb}$, which has a value in the range from a few to hundreds of V depending on the materials of the junction and their degree of hydration.

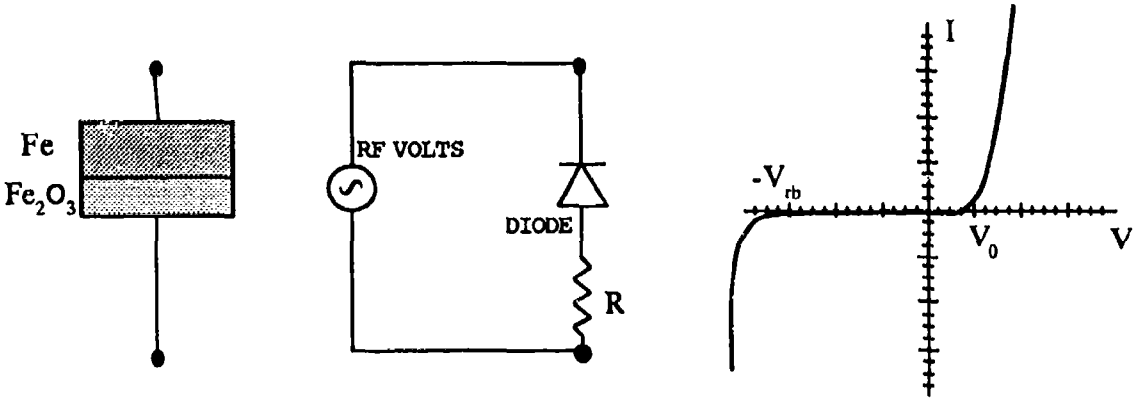


Fig. 3 - Rectifying metal semiconductor junction

Figure 4 shows the macro-equivalent circuit of a metal-semiconductor-metal (MSM) junction and its I-V curve. Breakdown occurs at $+(V_{rb} + V_0)$ and at $-(V_{rb} + V_0)$.

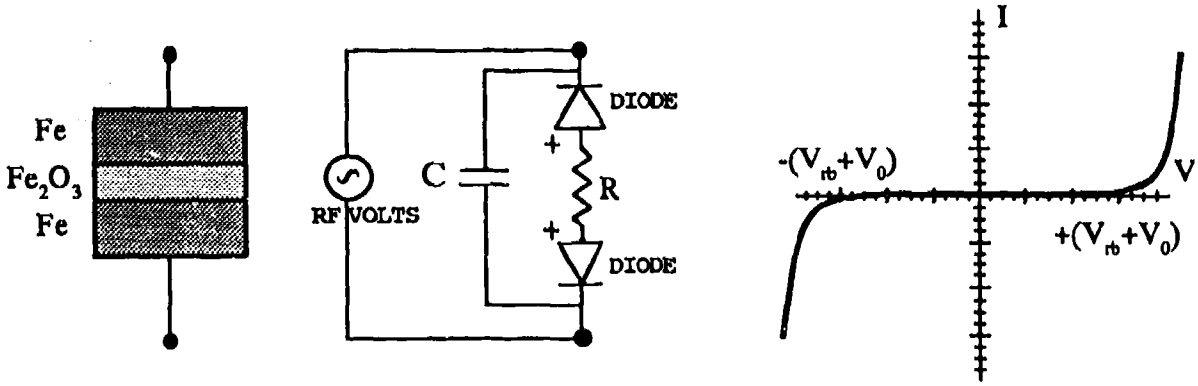


Fig. 4 - Metal-semiconductor-metal junction

This component is very nonlinear when it is driven by a strong signal. The typical electromagnetically active junction found in the Fleet is an MSM device in a very strong RF electromagnetic field. The semiconductor arises from oxidation of the metal surface before (or after) two metal pieces are brought into contact. Because the MS contact is used extensively in integrated circuit technology, the electrical properties of the MS contact are well understood [1, 2,6]. The properties of MS contacts vary widely, depending on the materials and dimensions described. First, consider some properties of the MS contact. Then we will apply these properties to the rusty bolt model.

The three types of MS contacts--ohmic, nonlinear tunneling, and rectifying--exhibit strikingly different behavior. The ohmic contact is generally formed by a metal and a highly doped (degenerate) semiconductor. The depletion layer (the physical separation between the majority carriers and the metal caused by the built-in potential at the junction) is so thin that the electrons tunnel through the barrier. When a potential is applied, the potential drop across the junction is negligible when compared to the ohmic drop in the semiconductor material. The rusty bolt does not exhibit ohmic behavior since the semiconductor materials involved are not degenerate. An ohmic contact would not produce IMI and is not relevant to this research.

A very thin layer of nondegenerate semiconductor (rust) between two metals, however, will also cause tunneling. In this case the electrons simply tunnel through the oxide layer because of the proximity of the metal pieces. The probability of tunneling decreases exponentially as the thickness of the oxide increases [1]. This tunneling process exhibits nonlinear behavior and produces a nonlinear resistance for oxide thickness up to 200 nm [1,3].

Oxide thickness greater than 200 nm produces two back-to-back rectifying MS contacts. A rectifying MS contact is formed between metal and iron oxides, $Fe_2O_3$ being the most common. The rectifying nature arises from the built in potential, because of the difference in work functions of the two materials. In the current-voltage relationship for the rectifying MS contact shown in Fig. 3, $V_o$ is the built in voltage, and $V_{rb}$ is the reverse breakdown voltage.

Figure 5 shows that the electrical model of the electromagnetically active junction consists of two back-to-back rectifying MS contacts.

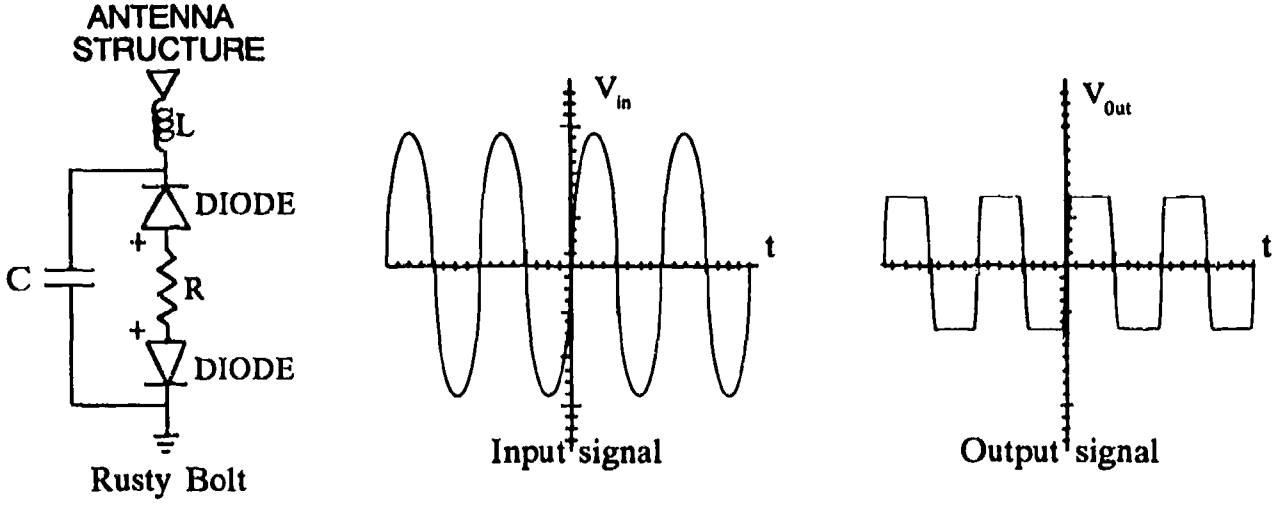


Fig. 5 - Rusty bolt aboard ship

The diodes are back-to-back because the top diode is due to a metal-semiconductor contact and the bottom diode is due to a semiconductor-metal contact. The resistance between the two diodes represents resistivity of the bulk semiconductor between the two metal pieces and is a function of the thickness of the oxide layer. The bulk semiconductor is that part of the $Fe_2O_3$ that is not an active part (depletion region) of either MS contact. The parallel capacitance is due to charge storage between the metal pieces and the diffusion capacitance of the two junctions. The inductor $L$ represents the lead inductance, which is usually small. However, aboard ship, if the antenna element of the circuit were a twisted or coiled steel cable, the inductance would be significant. This MSM contact is found between part of the superstructure that acts as an antenna and another part of the ship that acts as ground. A ladder might act as the antenna, and the deck might act as the ground. The MSM contact is a nonlinear, voltage limiting device. Because the diodes are back-to-back, little current flows through the rusty bolt until the voltage exceeds $V_{rb} + V_o$. Then the back-biased diode breaks down and the current is limited only by the small bulk resistance. Figure 4 shows that this results in a nonlinear voltage transfer characteristic. A Fourier analysis of the input waveform in Fig. 4 results in a single line at the RF frequency. However, because of the voltage limiting caused by the MSM contacts, a Fourier analysis of the output waveform results in a large number of harmonically related spectral components.

**Nonlinear behavior of this sort results in the generation of harmonics when a single RF carrier is transmitted. Intermodulation products are also generated when multiple carrier frequencies are present.**

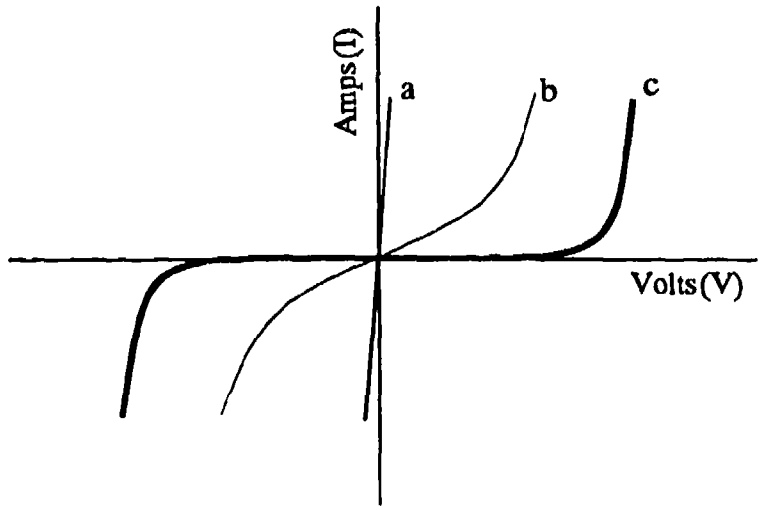


Fig. 6 - Basic I-V curves

The electromagnetic environment created aboard ship by rusty bolts is very complex. The fact that hundreds of rusty bolts can exist simultaneously contributes to the complexity. Another factor is the different modes in which rusty bolts can operate. Figure 6, curve a, shows that a new rusty bolt with a very thin layer of rust in the form of ferric oxide ($Fe_2O_3$) may operate as a linear resistor. Figure 6, curve b, shows that at the same time and in the same general area, a different rusty bolt with ferric oxide 100 nm thick may be operating in the tunneling mode as a nonlinear resistor. Also in the same area, there may be several rusty bolts with much thicker ferric oxide operating as MSM junctions with the current vs voltage characteristic seen in Fig. 6, curve c. There may also be rusty bolts composed of ferrous oxide (FeO) or ferric hydroxide [$Fe(OH)_3$] with similar characteristics, and air gaps that break down under strong signal conditions producing arcing and high levels of broadband noise. The most prevalent and stable electromagnetically active rusty bolts in the Fleet are likely to be of the type described by Figs. 4 and 6, curve c, which are equivalent.

## REQUIREMENTS FOR IMI REDUCTION

Attenuation requirements for the chemical suppression of IMI were developed from measurements of shipboard topside IMI levels for typical ships and the quasi-minimum-noise (QMN) levels at the receiving antenna [7]. Figure 7 shows measured data for these parameters. Ideally, the IMI should be reduced to the QMN level. Thus, it is desirable to attenuate the IMI at 2 Mhz by 29 dB and to attenuate the IMI at 30 MHz by 61 dB.

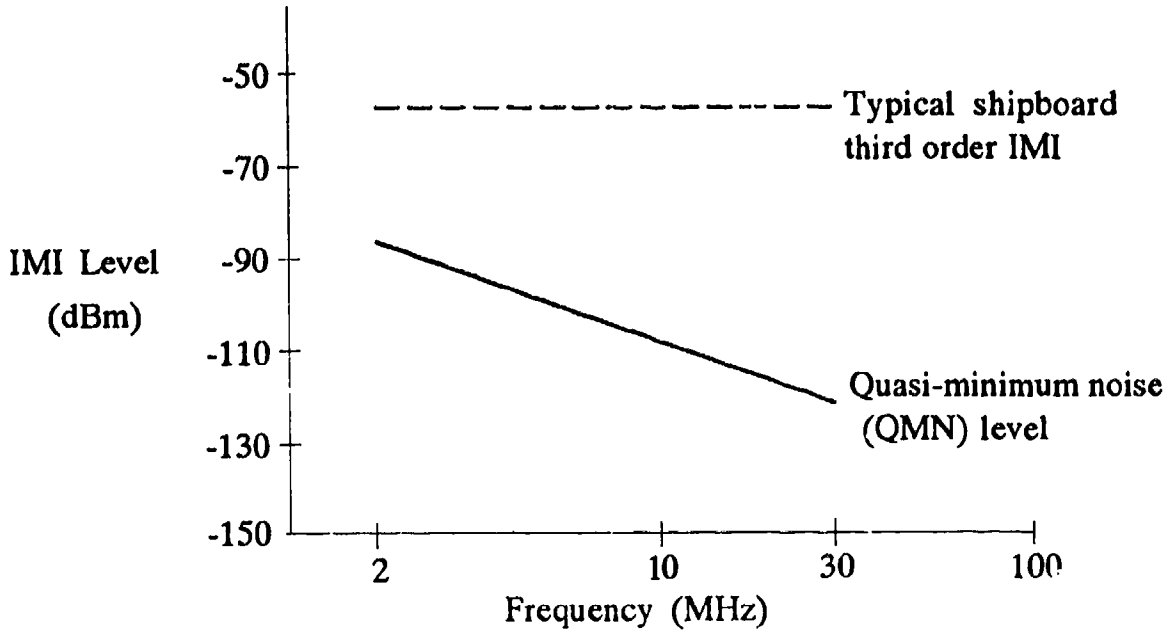


Fig. 7 - Typical shipboard third order IMI vs QMN level

Figure 4 shows that the electrical behavior of a rusty bolt is similar to that of two series-connected back-to-back semiconductor diodes. The MSM junction mixes the signals passing through the rusty bolt and generates IMI. The IMI will be suppressed if the current through the rusty bolt is reduced by a parallel low impedance path that has a linear current vs voltage characteristic, which can be achieved through the use of a "chemical shunt" to be described next.

## THE CHEMICAL APPROACH

### Interfacial Electrochemistry

The surfaces of even freshly polished iron or steel rapidly react with oxygen from the air so that the junction between two pieces of such very lightly oxidized steel can be considered to conform to the formulation FeO or $Fe(OH)_2$ in humid or moist conditions. The oxide form that we tested in the laboratory was nonstoichiometric (approximately $FeO_{0.95}$) so that it had an excess of holes and, therefore, was a p-type semiconductor. The degree of hydration of such dry, rusty-bolt junctions may, therefore, affect the hole carrier density in the semiconducting layer.

In laboratory tests, the degree of nonlinearity of the simulated junction is affected by mechanical pressure. Light contact pressure between the two metal plates results in the maximum degree of nonlinearity. However, such junctions are mechanically unstable and are not

a realistic representation of an electromagnetically active junction in a shipboard environment. Therefore, the contact pressure is adjusted in the laboratory to give a stable, nonlinear characteristic.

Within each of the metal-to-semiconductor interfaces in the Fe-O-Fe junction, there is an interfacial potential difference for electrons in the different phases. The inherent electric field gradient $X_{eq}$ across the interfacial region results in the familiar exponential, band-bending phenomenon in the semiconductor, that can lead to a Garrett-Brattain [8] space-charge depletion layer. The degree of conductivity across this layer and its width $l$ are intimately dependent on the density of charge carriers (electrons or holes) available within the semiconductor. $FeO_{0.95}$ is a relatively poor conductor, relying on electron-hopping from $Fe^{2+}$ to $Fe^{3+}$ cations (valence band) for conduction. This type of conduction is commonly known as hole or p-type conduction.

At equilibrium, there is no net electron transfer across the metal-to-semiconductor interface. However, the interfacial potential is maintained by a dynamic equilibrium of equal but opposite charge transfers. These small equilibrium currents within the interface are known as the exchange current density $i_o$, which represent first-order kinetic processes in each direction. The rate of charge transfer (current) at equilibrium determines the electrical conduction characteristics of the interface under the application of an external electric field $X$. Under the influence of a voltage source, the interfacial potential will be displaced from the equilibrium value to an extent dependent on $i_o$. Therefore, an overpotential ($\nu = E - E_{eq}$) will develop as a consequence of the net current. Nonlinear I-V response curves are observed when the current demand exceeds the inherent current supply $i_o$ in the interface.

Therefore, each metal-to-semiconductor interface is expected to display exponential I-V curves according to the Butler-Volmer equation [8]:

$$i_{obs} = i_o \ [\exp(-anf\nu) - \exp((1 - a)nf\nu)],$$

where

$i_o$ is the inherent exchange current density in the semiconductor;
a is 0.5 (if a symmetrical activation barrier to charge transfer is assumed);
n is the number of electrons in the rate determining step;
$f$ equals F/RT (38.92 $V^{-1}$ at 298K) and;
$\nu$ is the activation overpotential, $\nu = [E - E_{eq}]$, where $E_{eq}$ = Fermi level).

Figure 8 depicts the resulting hyperbolic sine function for charge transfer across each interface for five values of the exchange current density ($i_o$ = 1E-6,...,1E-2) plotted on a scale of 1 mA. Although each of these curves is equally nonlinear (they differ only by a scale factor), the apparent linearity for the same small current across the interface is greatly improved with increasing exchange current density, *i.e.* the junction appears to be most linear when the current demand is much smaller than the current supply in the semiconducting layer.

The experimental, small signal I-V curves for the Fe-O-Fe type junctions closely resemble those predicted by the simple Butler-Volmer equation above, which formally applies

only to a single interface where mass transport (for systems requiring Faradaic oxidation-reduction or solid-state ion migration) is not a limiting factor. When such factors do limit the charge transfer across the interface, the general I-V equation will describe the behavior of each interface [5]:

$$i_{obs} = i_o[C_{ox}(0,t)/C_{ox}^*\exp(-anfv) - C_{red}(0,t)/C_{red}^*\exp((1-a)nfv)],$$

where

$C_{ox}^*$ is the bulk concentration of the oxidized species;
$C_{red}^*$ is the bulk concentration of the reduced species;
$C_{ox}(0,t)$ is the surface concentration of the oxidized species;and
$C_{red}(0,t)$ is the surface concentration of the reduced species.

The concentration ratio terms limit the maximum current producing characteristic S-shaped diffusion limited plateau curves from the modified Butler-Volmer equation. The concentration terms could equally apply to species diffusing to the metal surface to undergo Faradaic redox reactions or to ions migrating through the oxide layer under the influence of the extremely high field gradient in the junction (~$10^6$ V /cm). Obviously, the general I-V curve must be solved numerically since the surface concentrations are time dependent. Such diffusion limited I-V curves are observed occasionally during laboratory setup of Fe-O-Fe junctions, but, for the most part, the simple Butler-Volmer equation adequately represents the electrical behavior of these junctions. Thus, there is a good physical and chemical basis for the nonlinear I-V properties exhibited by these Fe-O-Fe junctions.

*Characteristics of Laboratory Nonlinear Junctions*

Laboratory scale rusty-bolt junctions were prepared from lightly abraded pieces of steel bar sandwiched together in a hand-adjusted vise. Under light contact pressure, relatively stable nonlinear junctions can be prepared while observing a 60 Hz I-V trace. The electronic conduction of this array of Fe-O-Fe junctions can display quite similar response shapes to those predicted by the Butler-Volmer equation [6] (Fig. 8). However, the voltage limits achieved in the experimental device before current limiting sets in are about ten times larger than those predicted by the Butler-Volmer equation. This arises from the difference between the applied voltage and the actual overpotential appearing across the ms junctions' space-charge region. The remainder of the applied voltage is dropped across ohmic losses in the device and external components in the measurement apparatus. Therefore, some assumptions about the overpotential have to be made to model the electrical performance of the test device.

*Modeling of IMI Production from Nonlinear Junctions*

For any model of the interfacial charge transfer kinetics to be successful, it must predict the experimental observations of odd-order only intermodulation products with the correct relative amplitude ratios. The first requirement can be met with any symmetrical, odd transfer

function. The second requirement can be investigated by using numerical calculation of the amplitudes with Fourier Transform analysis of the current waveform through the device. The input waveform to the experimental device consisted of two, equal amplitude sine waves, crystal locked to 2.000 and 2.828 MHz. The choice of frequency ratio (1.414) ensures that the products

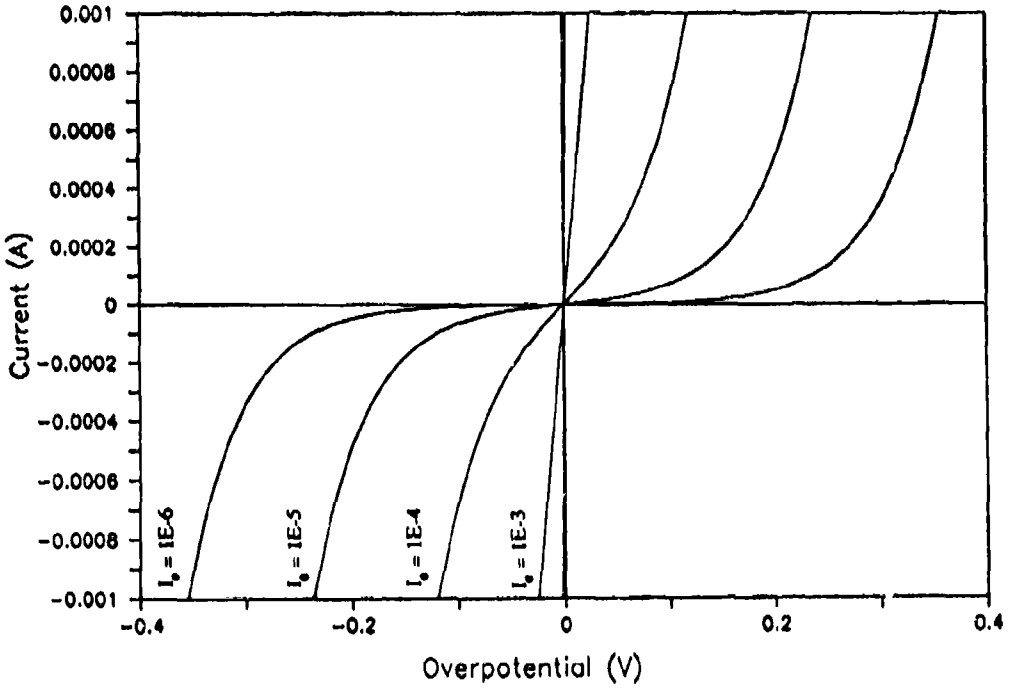


Fig. 8 - Butler-Volmer equation; no mass transfer limit

of individual orders can be resolved spectrally. This implies that a large number of cycles are required (707) before coincidence of the two sine waveforms occurs. Therefore, Fourier domain analysis must be applied to a large number of multiples of the 2 Mhz waveform to avoid serious truncation errors that produce a large number of artifacts. This allows a 16K Fourier transform to cover the desired frequency range of 0 to 28.5 MHz, comparable to the range of observed IMI products in the experimental apparatus.

The calculations of the synthesized waveforms and their spectral distributions were performed by using programs written in Array BASIC, an highly optimized language embedded within the commercial software package Spectra Calc for use on IBM PC compatible computer systems. In this language, equations are automatically calculated for a whole array of independent variables without the need for point-by-point loops. This results in exceptionally fast execution for numerical calculations. Similarly, a single RFFT *array* command performs a complete real FFT on an array.

For single tone response tests, the Butler-Volmer equation was used to transform a sinewave input signal to a predicted current output waveform as a function of input amplitude and exchange current density. Figure 9 shows a typical output waveform with the corresponding real FFT analysis depicted in Fig. 10 for an input signal of 0.4 V (p-p) with the exchange current

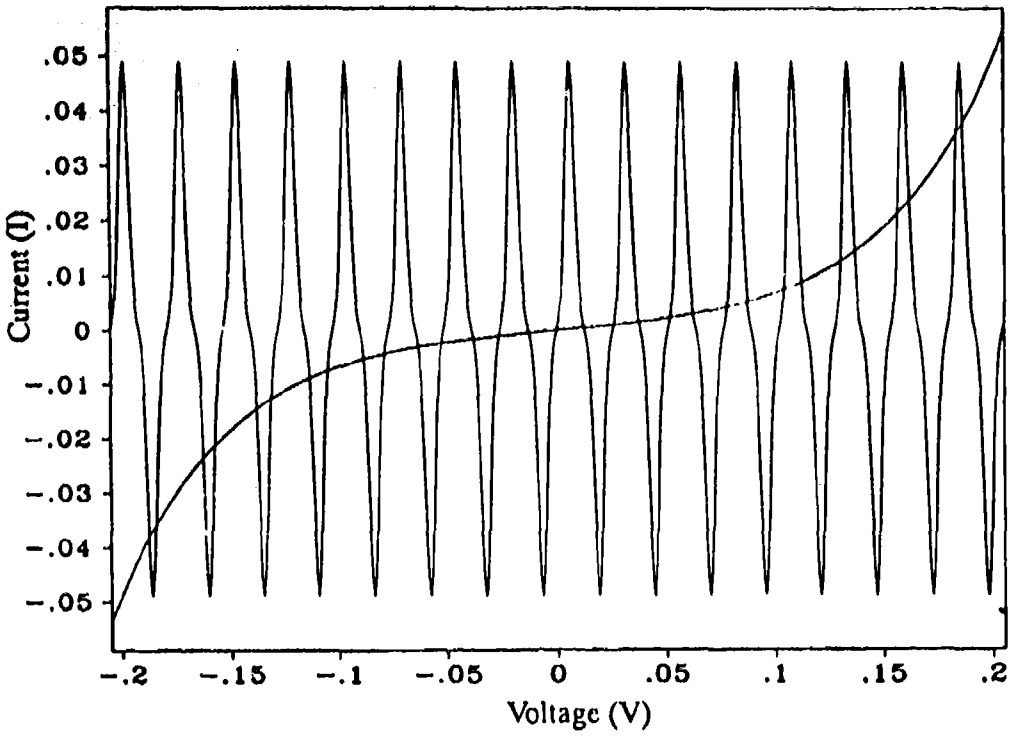


Fig 9 - Input waveform: 0.4V, (p-p) sine wave

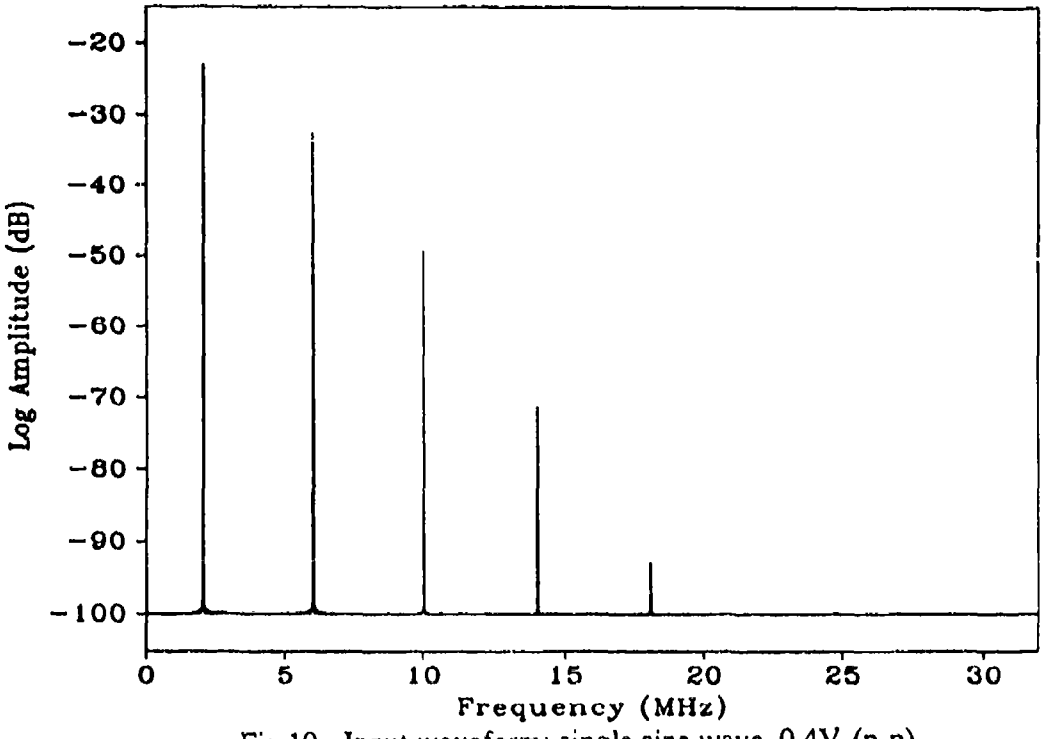


Fig 10 - Input waveform: single sine wave, 0.4V, (p-p)

density set to 1E - 3. The latter value was chosen to approximately match the conduction characteristics of the Fe-O interface. As expected, only odd-order harmonics were generated from the Butler-Volmer equation. This calculation was performed on 32 cycles of the input sinewave by using a 1K real FFT. The execution time was less than 2 s for a 16 MHz IBM PS/2 Model 80 computer system. The amplitude distribution diminishes faster than exponentially with increasing order so that no harmonics above the 11th order are discernible on the scale plotted in Fig. 10. The higher order harmonics can be easily produced by increasing the amplitude of the input signal across the interface into the most nonlinear portion of the Butler-Volmer I-V curve. Similarly, reducing the amplitude of the input waveform to 0.01 V (p-p) results in no significant harmonic generation.

Two-tone response tests were performed in a similar manner by using a 577-cycle (2 MHz) period to calculate an accurate input waveform. A Fourier domain analysis of this input waveform showed that there were only very small artifacts produced by truncation errors (Fig. 11). However, to avoid any spurious responses in the real FFT analysis, the input waveform was Fourier domain filtered by using a boxcar envelope detector (Fig. 12) before being applied to the Butler-Volmer response function with $i_o$ set to 1E - 3. The resulting current output waveform (Fig. 13) was then transformed to display the IMI products (Fig. 14). The amplitude distribution of the IMI products was found to be very similar to experimental measurements, and the frequencies of all components exactly matched those calculated for odd-order intermodulation. A listing of the expected frequencies up to the 19th order is given in the Appendix.

The components above the 11th order were found to be vanishingly small, as observed in the experimental test device. On board Navy ships it is not uncommon to observe IMI products up to the 49th order, while the requirements for adequate standards of communications could be met by suppression of the 19th order components to -100 dBm. The generation of such high orders of IMI products requires large overpotentials across the rusty-bolt interfaces, implying that much larger current densities occur in the nonlinear junctions on board the Naval vessels. This arises from the appearance of the powerful transmitters as infinite current sources with the ability to generate large amplitude signals across the nonlinear junctions. It would be difficult to drive experimental junctions at these levels in the laboratory.

*Summary of Techniques for Modeling of Nonlinear Junctions*

The ability to modify and control the oxides between metal surfaces is critical for ensuring linear conduction of the MOM junctions. By their nature, such junctions are usually depleted of mobile charge carriers and, therefore, exhibit nonlinear I-V behavior. Through appropriate chemical treatments it is possible to modify the interfacial oxides to increase the availability of charge carriers, thus increasing the exchange current density and reducing the width of the space-charge region. This lowers the overpotential across the interface alleviating some of the nonlinearity of the junction.

## Selection of Materials

A chemical formulation intended to shunt a rusty bolt junction must be able to penetrate or remove the metal oxide, must have low impedance, and must carry significant current without

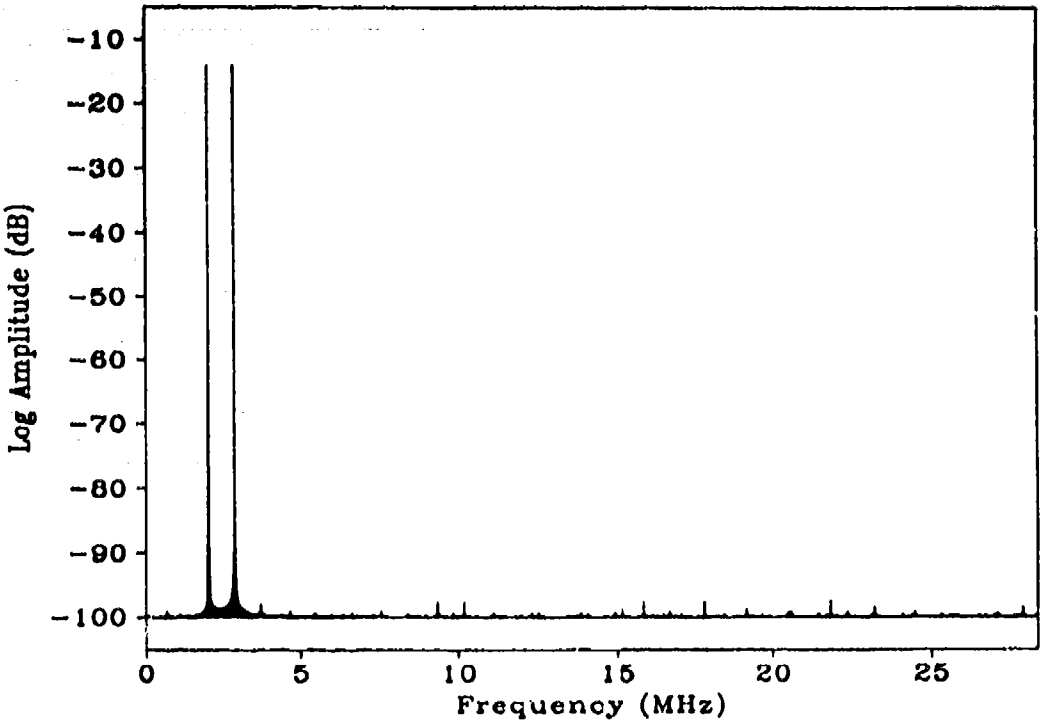


Fig. 11 - Input waveform: two sine-wave composite, 0.4V (p-p)

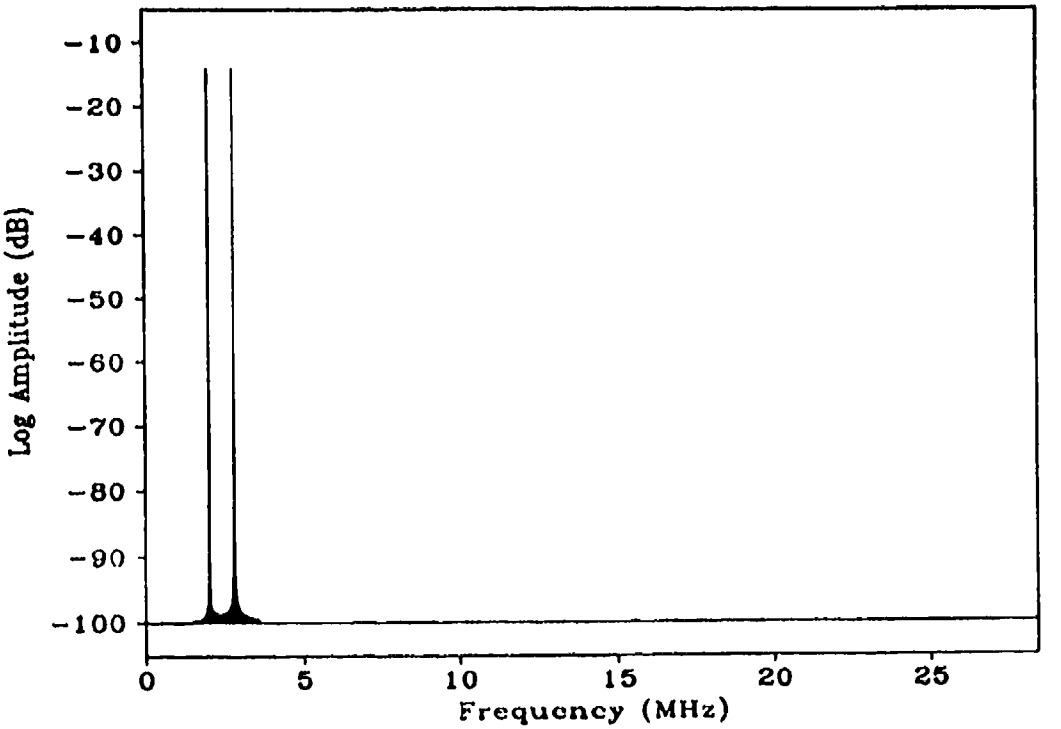


Fig. 12 - Input waveform: two sine-wave composite, 0.4V (p-p)

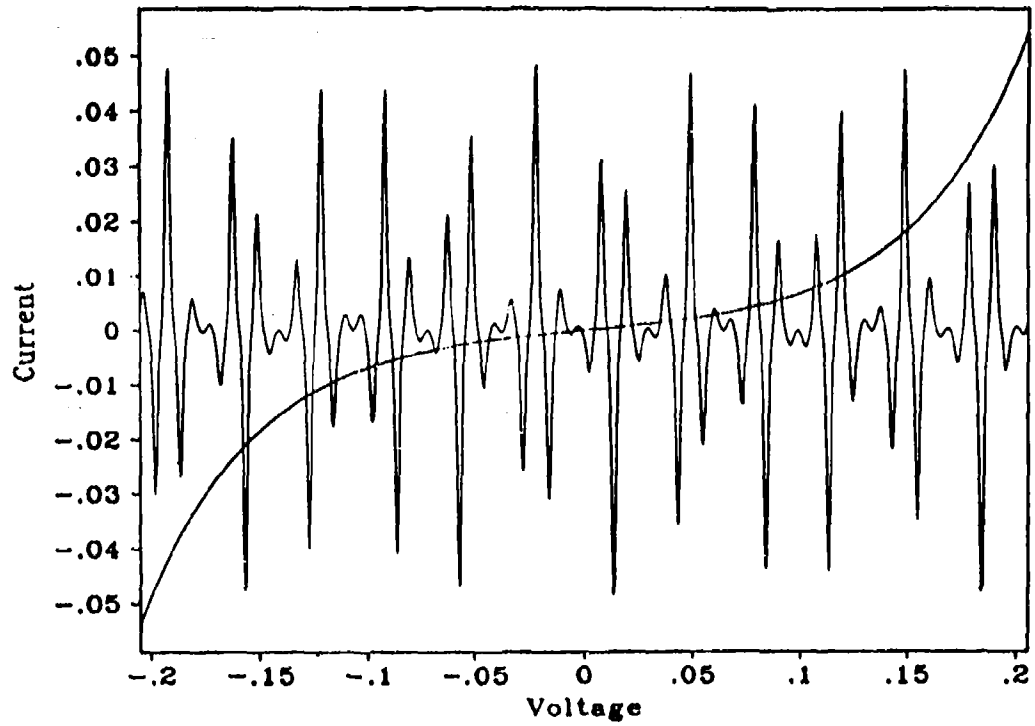


Fig. 13 - Input waveform: two sine-wave composite, 0.4V (p-p)

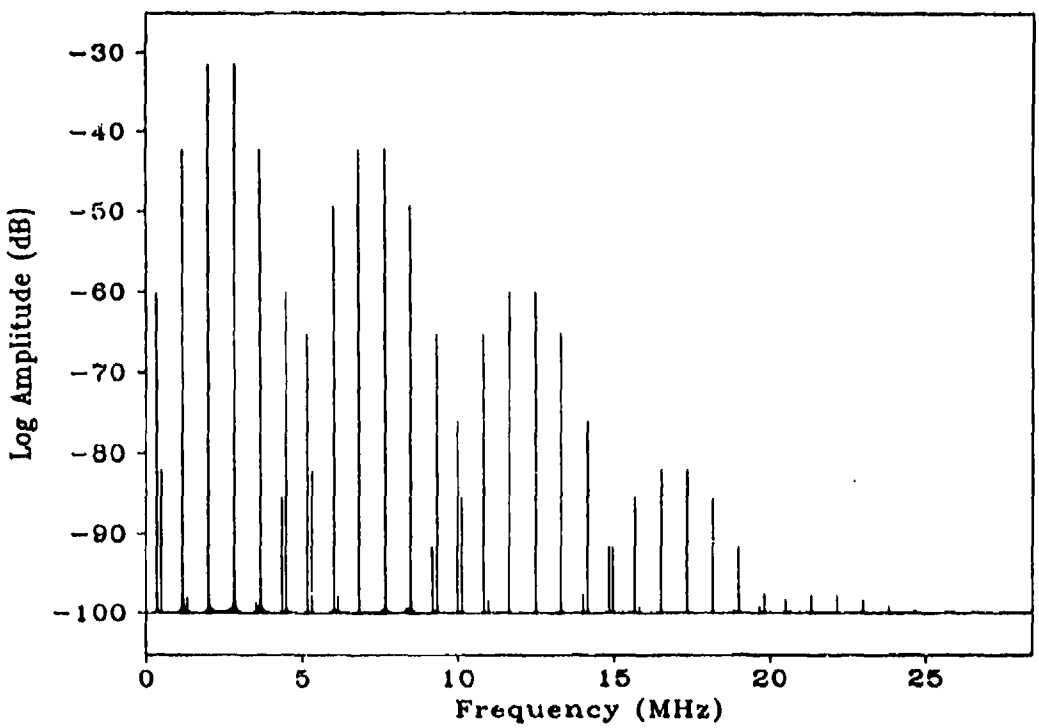


Fig. 14 - Input waveform: two sine-wave composite, 0.4V (p-p)

degradation. This material must also protect the surfaces from further corrosion, adhere well to the metal surfaces, be somewhat elastic, and be chemically stable. The low impedance requirement can best be met by producing a material with both low resistance and low reactance. The low resistance requirement can be met by developing formulations that contain zero valent metals or incorporate zero valent metals by reducing the metal oxides present on the surface. The low reactance requirement can be achieved by developing formulations with high dielectric constants. To provide a low impedance path, the metal oxide must be removed or modified and the metal surface protected from further corrosion. This can be accomplished chemically without corrosion of the metal surface by binding the metal atoms with a chelating agent and incorporating a general acid catalyst to accelerate the rate of oxide dissolution.

The following properties will decrease corrosion: (a) tight adherence of the IMI reducing paint to the metal surface to exclude oxygen, (b) incorporation of a chemical reducing agent to scavenge oxygen, and (c) a protective film.

A chemical reducing agent can also reduce metal ions from the oxide to zero valent metal, thus producing a conducting mixture. The effectiveness of this approach depends on the relative reduction and oxidation potentials of the metal oxide and the reducing agent. Good adherence of a material containing a polymer to a metal surface is best achieved by thoroughly removing the oxide coating. In addition, an elastic formulation, obtained by use of elastomeric materials, will prevent breaking of the bond between the material and the metal surface during slight flexing of the junction.

Polyvinylpyrrolidone (PVP) was selected for inclusion in several candidate formulations to provide the needed viscosity change once the material is in the junction. PVP cross-polymerizes by binding or chelating metal ions through the nitrogens and oxygens in different chains [9]. The result is a large increase in viscosity in the presence of metal oxides. As a weak chelating agent, PVP assists in surface cleaning [3]. In addition there is evidence [10] that PVP will reduce $Fe^{3+}$ to $Fe^{2+}$ and change the reduction potential of $Fe^{2+}$ by complexing, to allow reduction to $Fe^{0}$ by mild reducing agents thus providing conductivity.

"Adiprene"™, another compound selected for inclusion into candidate formulations, is a liquid urethane elastomer that is cured in these applications by the reaction of water from the air and hydrous metal oxides with terminal isocyanate groups on the polymer [10]. In addition to a change from low to high viscosity as for PVP, the product contains amine groups that bond metal ions, assisting in surface cleaning. The elasticity of "Adiprene" polymers increases the chemical stability of the material on exposure to environmental stress.

Erythorbic acid is another chemical chosen for inclusion in the IMI suppressing formulations. It is a low cost reducing agent or antioxidant that also complexes $Fe^{2+}$, $Fe^{3+}$, and other metal ions. It will reduce $Ag^{+}$ rapidly to elemental silver, $Cu^{2+}$ to $Cu^{1+}$, and finally to $Cu^{0}$ with slight heating and efficiently scavenges oxygen to inhibit further surface corrosion. Conductivity is provided by the zero valent metals. Erythorbic acid served as an efficient general acid catalyst in the protonation and removal of metal oxides. Citric acid was also investigated.

EDTA was chosen as a component for IMI suppression because of its very strong affinity for $Fe^{3+}$, $Fe^{2+}$, and many other metal ions. Other compounds shown in Table 1 were selected for their high dielectric constants (ethylene glycol, water), or their solvent and paint penetration properties.

Table 1 - Shipboard 5th-order IMI Suppression*

| Material type | Components | IMI Suppression (Db) |
|---|---|---|
| A | AgNO, PVP, $H_2O$ Erythorbic Acid | 13 |
| E | PVP, $Na_4EDTA$,$H_2O$ Erythorbic Acid, Ethylene Glycol | 27 |
| I | Cu(pyrolidine)$Cl_2$ PVP, Ethelene Glycol | 12 |

* Many formulations were tested. Table 2 reports the best formulations developed and some of the simpler mixtures that lead to these formulations. Although many mixtures have been evaluated, those in Table 2 represent the principal chemical approaches used.

## EXPERIMENTAL PROCEDURES

### Laboratory Experiments

A laboratory test was conducted to simulate the use of a candidate chemical material to by-pass a rusty bolt. This was accomplished by shunting an MSM junction in the laboratory with discrete resistors and then repeating the process with discrete capacitors. Capacitors can be used as shunts because at HF, they provide a low reactance. It was found that IMI suppressions in the range of 40 to 50 dB were achieved by shunting the rusty bolt path with chemicals that duplicate the linear low impedance characteristics of the discrete components. The capacitive contribution becomes more pronounced at higher frequencies.

Numerous chemical formulations were developed that satisfied some or all of the IMI reducing requirements. To achieve reproducibility and comparability, experiments were conducted by creating rusty bolts with approximately the same stable nonlinearity and resistance characteristics as determined from the I-V curve. The candidate material was added, the reduction in IMI intensity was determined, and the entire experiment was repeated several times to determine the confidence level justified by the measurements.

A reproducible method was required to measure IMI reduction by candidate formulations. This requirement was met by designing a laboratory rusty bolt simulation system having a two-frequency transmitter, a rusty bolt, and a receiver. The transmitter was a two-tone test

generator. The rusty-bolt consisted of two pieces of steel each of which measured 7 cm in length and had a crossection measuring 3 mm on each side.

TABLE 2 - Reductions in 3rd-Order IMI for Formulations Applied to Steel-Steel Nonlinear Junctions

| TYPE | COMPONENTS | (%) | Delta IMI (dB) at 6.828 mHz |
|---|---|---|---|
| A | $AgNO_3$ | 6 | |
| | Erythorbic Acid | 13 | |
| | PV | 13 | 42.0±1.0 |
| | $H_2O$ | 68 | |
| B | PVP | 10 | 12.8±0.3 |
| | $H_2O$ | 90 | |
| C | PVP | 6 | |
| | Ethylene Glycol | 47 | 27.9±0.4 |
| | $H_2O$ | 47 | |
| D | PVP | 50 | |
| | Erythorbic Acid | 40 | 29.1±0.4 |
| | Ethylene Glycol | 10 | |
| E | PVP | 10 | |
| | Erythorbic Acid | 65 | |
| | $Na_4EDTA$ | 7 | 46.1±5.0 |
| | Ethylene Glycol | 7 | |
| | $H_2O$ | 11 | |
| F | Adiprene | 50 | |
| | Citric Acid | 50 | 8.3 ±0.6 |
| G | Adiprene | 75 | |
| | $Na_4EDTA$ | 25 | 25.8±0.5 |
| H | Adiprene | 50 | |
| | Citric Acid | 25 | 35.2±0.6 |
| | Erythorbic Acid | 25 | |
| I | Cu(pyrolidine)$Cl_2$ | 20 | |
| | PVP | 5 | 51.0±3.0 |
| | Ethylene Glycol | 75 | |

Note: The ± numbers indicate the range of results for the 10 test repetitions for each formulation tested.

The metal pieces were held in an orthogonal position and in physical contact. A pin vise was used to adjust the pressure at the junction between the two pieces of steel. The receiver was an HP 8966A spectrum analyzer with an HP 9825 controller. The spectrum analyzer was programmed to scan from 0 to 30 MHz, simulating a communications receiver and measuring and displaying the amplitude level of each IMI frequency component. This procedure was performed both before and after the junction was doped with each candidate material. The HP 9825 controller calculated the IMI frequencies, programmed the spectrum analyzer to operate as a shipboard communications receiver, tuned the simulated receiver to the IMI frequencies, and measured the relative IMI power levels.

Figure 6, curve b, shows that the laboratory simulator operates in the tunneling junction mode with the nonlinear resistance characteristic described earlier, while the typical shipboard rusty bolt operates in the MSM junction mode driven beyond breakdown as shown in Fig. 6, curve c. To validate the tunneling junction method of evaluating materials in the laboratory, it was necessary to test the same materials on shipboard rusty bolts.

### Shipboard Testing

The IMI suppressing formulations were tested on an aluminum superstructure ship and on a steel superstructure ship. On both ships, the tests were performed directly below the transmitting antennas. Standard NAVSEA procedures for conducting shipboard electromagnetic interference surveys (MIL-STD-1605) were employed. Two HF transmitters were coupled to the same antenna through a multicoupler. Figures 15 through 18 present IMI measurements made by the Shipboard Electromagnetic Compatibility Improvement (SEMCIP) team aboard the USS *Wasp* (LHD-1) and reported to NAVSEA by Mr. George Johnson of Eldyne Inc. These data provide an elegant display of a serious and currently unsolvable problem in the Fleet. The ships' receivers and the Automated System for Intermodulation Assessment (ASIA) were used to identify the IMI level being generated. Broadband noise (BBN) measurements were also made. IMI has also been measured aboard ship by NRL personnel by using laboratory test equipment.

## RESULTS

### Laboratory Results

Table 2 shows the results of laboratory testing. Several materials tested (A,E, and I) provide more than 40 dB IMI reduction at 6 MHz.

### Shipboard Results

First, subjective measurements were made on each formulation. When these were applied to actual shipboard rusty bolts, the IMI was reduced to barely audible or undetectable levels for 9 of the 10 formulations. The 10th formulation could not penetrate to the exact physical location of the nonlinear junction. Three of the materials were tested aboard ship by using laboratory equipment. (The results of these tests appear in Table 1.)

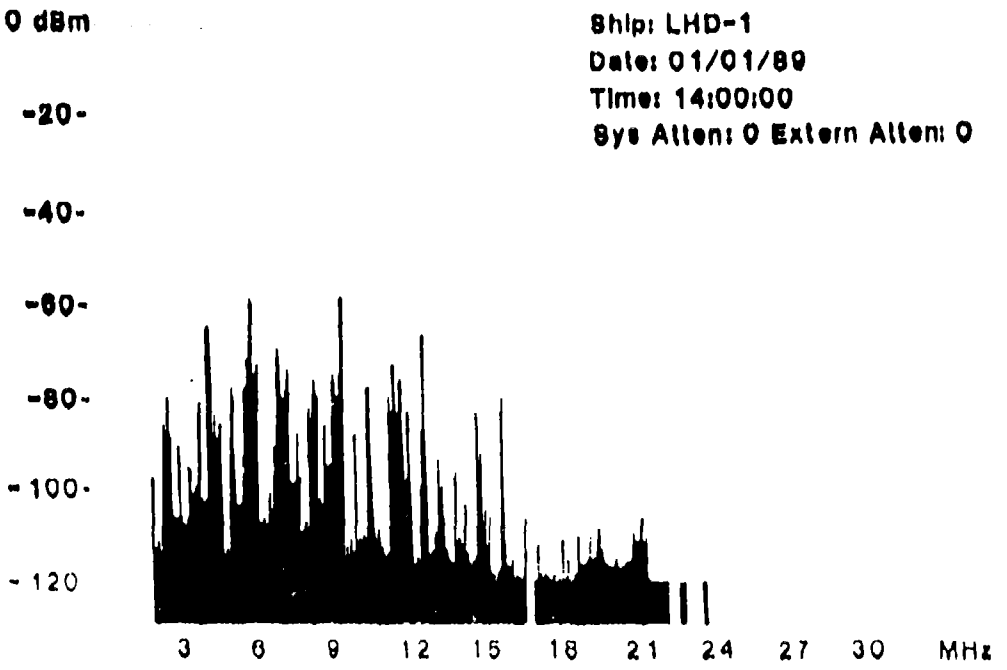


Fig. 15 - Atmospheric signal strength

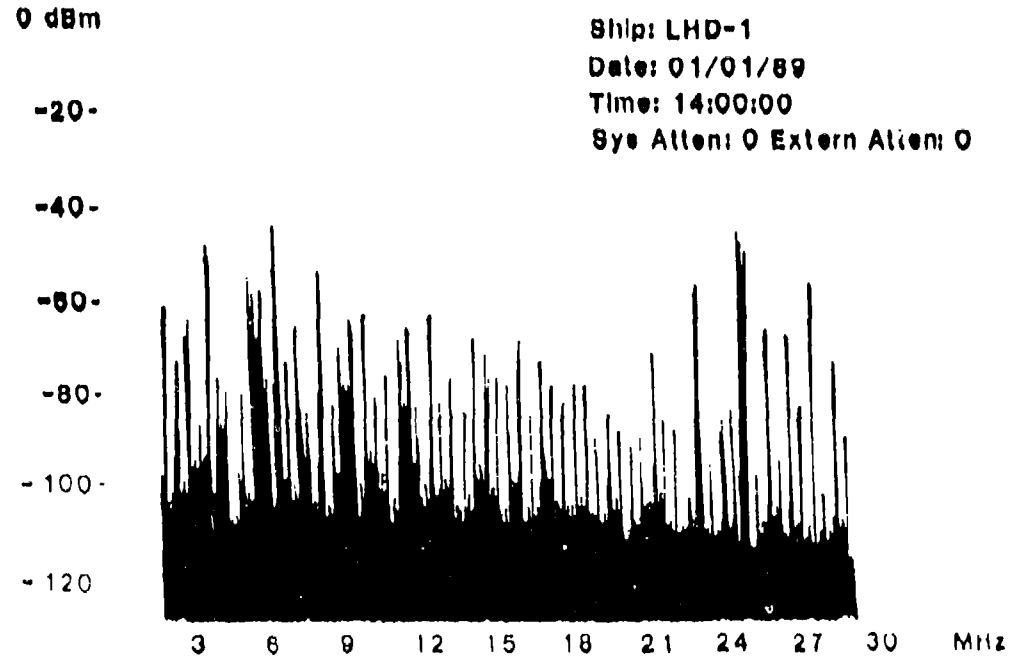


Fig. 16 - IMI signal strength

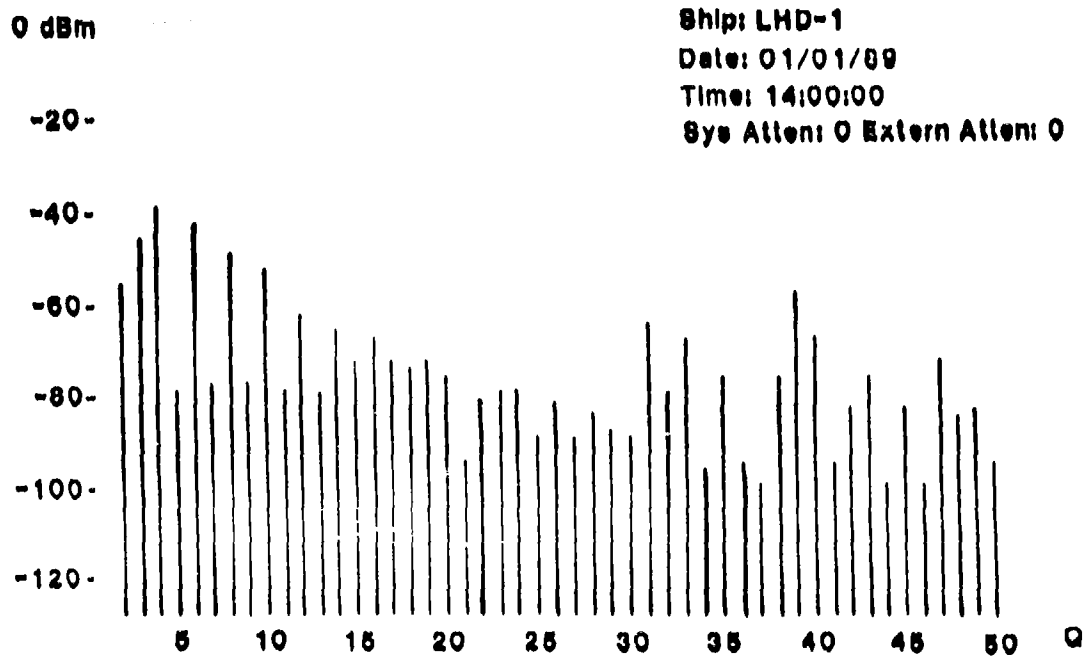


Fig. 17 - IMI amplitude vs order

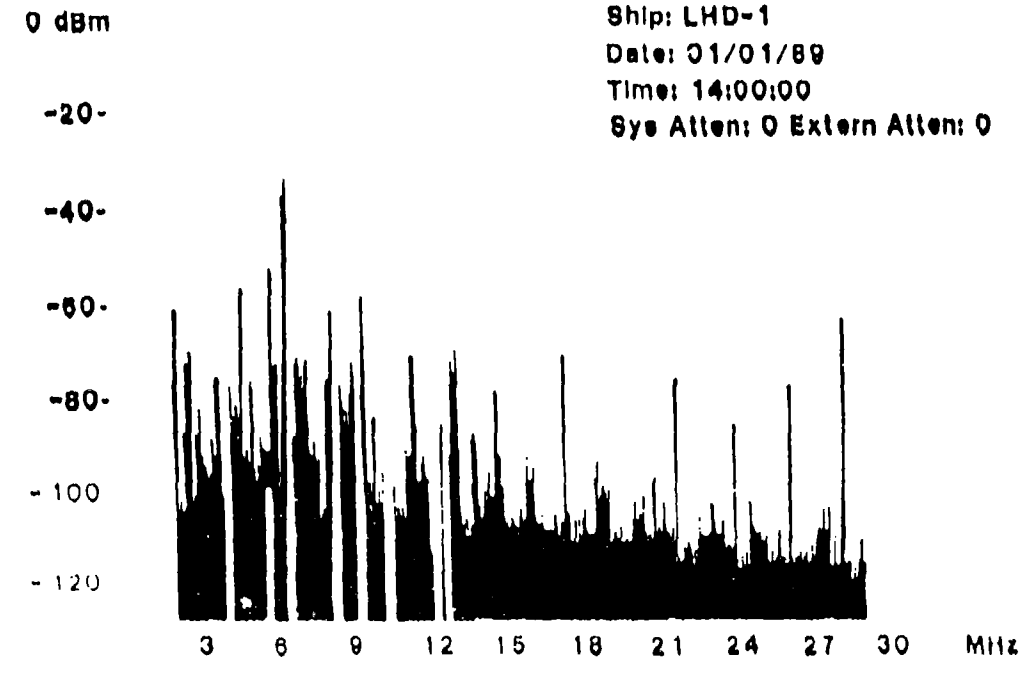


Fig. 18 - BBN signal strength

The shipboard results were encouraging. However, further operational testing is required to provide quantitative results that are comparable to the laboratory tests (i.e., measure the same IMI orders) and to establish the effectiveness of the various materials as additives to paints and greases during extended operational use.

## CONCLUSIONS

Formulations A, E, and I from Table 2 provide the best IMI reduction at HF under laboratory and shipboard conditions. Formulations A and I were patented by The Naval Research Laboratory [11,12]. Both have the following effects on MSM junctions:

- Chelate the rust-causing ferric ion and incorporate it into a polymer.
- Change the oxidation state of the metal to increase conductivity.
- Prevent further corrosion by incorporating a chemical reducing agent.
- Preserve the structural integrity of the metal-to-metal junction.
- Provide multiple conductive paths for IMI reduction.

The best materials tested (A, E, and I) have the following chemical constituents: a metal chelating agent, a high dielectric constant solvent, a polymerizing bonding agent, and a reducing agent.

Additional experimentation is required to further refine the formulations and develop IMI-reducing paints and greases based on the optimized materials. Based on laboratory and shipboard test results, the two most promising formulations were chosen for additional shipboard testing and incorporation into paints and lubricants. These materials have been used as additives to the Navy's haze gray paints (FEDSPEC TT-E-490-E) and lubricants for exposed surfaces (MILSPEC MIL-G-18458) to reduce IMI. NAVSEA Application Instruction S9086-VD-STM-000/CH-631 has been developed to incorporate these materials into the FEDSPEC TT-E-490-E haze gray paint. An application instruction is also needed for use with the MILSPEC lubricant MIL-G-18458.

## REFERENCES

1. R. S. Muller, and T. I. Kamins, *Device Electronics for Integrated Circuits*, 2nd ed. (John Wiley & Sons, N. Y., 1986).

2. L. Solymar, and D. Walsh, *Lectures on the Electrical Properties of Materials*, 3rd ed. (Oxford University Press, N. Y., 1984).

3. M. Sze, *Physics of Semiconductor Devices*, 2nd ed. (John Wiley & Sons, N. Y., 1981).

4. J. L. Moll, *Physics of Semiconductors* (McGraw-Hill Inc, N.Y., 1964).

5. R. A. Greiner, *Semiconductor Devices and Applications* (McGraw-Hill Inc, N. Y., 1961).

6. J. O. Bockris and A. K. N. Reddy, *Modern Electrochemistry*, Vol.2 (Plenum Press, N.Y., 1970), Chs 8,9, and 11.

7. G. C. Salisbury, "Topside Intermodulation Interference Aboard USS *Mount Whitney* (LCC-20), USS *Blue Ridge* (LCC-19), and USS *Iwo Jima* (LPH-2)," NELC Tech Doc 206, Naval Electronics Laboratory Center, San Diego, Cal., December 1972.

8. A. J. Bard, and L. R. Faulkner, *Electrochemical Methods* (John Wiley & Sons, N.Y., 1980), Ch. 3.

9. R. Panayappan and J. C. Cooper, "Preparation and Properties of Some Transition Metal Pyrrolidine and Pyrrolidone Complexes," 17th Middle Atlantic Region Meeting, Amer. Chem. Soc., Apr. 6-8, 1983.

10. G. Odian, "Basic Concepts in Elastomer Synthesis; Elastomers and Rubber Elasticity," ACS Symposium Ser. 193, J. Mark and J. Lal, eds.,1982, pp. 27-29.

11. J. C. Cooper, "Chemical Bonding Agent for the Suppression of Rusty Bolt Intermodulation Interference," U.S. Patent 4,582,724, 1986.

12. R. Panayappan and J. C. Cooper, "Rusty Bolt Intermodulation Interference Reducer," U.S. Patent 4,591,510, 1986.

# Appendix

## EXPECTED IMI FREQUENCIES TO THE 19TH ORDER

| ORDER = 1 | ORDER = 3 | ORDER = 5 | ORDER = 7 | ORDER = 9 |
|---|---|---|---|---|
| 2.000 | 1.172 | 0.343 | 0.485 | 1.314 |
| 2.828 | 3.657 | 4.485 | 4.343 | 3.515 |
| 0.000 | 6.000 | 5.172 | 5.314 | 6.142 |
| 0.000 | 6.828 | 9.314 | 9.172 | 8.343 |
| 0.000 | 7.657 | 10.000 | 10.142 | 10.971 |
| 0.000 | 8.485 | 10.828 | 14.000 | 13.172 |
| 0.000 | 0.000 | 11.657 | 14.828 | 15.799 |
| 0.000 | 0.000 | 12.485 | 14.971 | 18.000 |
| 0.000 | 0.000 | 13.314 | 15.657 | 18.828 |
| 0.000 | 0.000 | 14.142 | 16.485 | 19.657 |
| 0.000 | 0.000 | 0.000 | 17.314 | 20.485 |
| 0.000 | 0.000 | 0.000 | 18.142 | 20.627 |
| 0.000 | 0.000 | 0.000 | 18.971 | 21.314 |
| 0.000 | 0.000 | 0.000 | 19.799 | 22.142 |
| 0.000 | 0.000 | 0.000 | 0.000 | 22.971 |
| 0.000 | 0.000 | 0.000 | 0.000 | 23.799 |
| 0.000 | 0.000 | 0.000 | 0.000 | 24.627 |
| 0.000 | 0.000 | 0.000 | 0.000 | 25.456 |

FIG. A1 - Odd intermodulation product frequencies by order

| ORDER = 11 | ORDER = 13 | ORDER = 15 | ORDER = 17 | ORDER = 19 |
|---|---|---|---|---|
| 2.142 | 1.858 | 1.029 | 0.201 | 0.627 |
| 2.686 | 2.971 | 3.799 | 4.627 | 4.201 |
| 6.971 | 6.686 | 5.858 | 5.029 | 5.456 |
| 7.515 | 7.799 | 8.627 | 9.456 | 9.029 |
| 11.799 | 11.515 | 10.686 | 9.858 | 10.284 |
| 12.343 | 12.627 | 13.456 | 14.284 | 13.858 |
| 16.627 | 16.343 | 15.515 | 14.686 | 15.113 |
| 17.172 | 17.456 | 18.284 | 19.113 | 18.686 |
| 21.456 | 21.172 | 20.343 | 19.515 | 19.941 |
| 22.000 | 22.284 | 23.113 | 23.941 | 23.515 |
| 22.828 | 26.000 | 25.172 | 24.343 | 24.770 |
| 23.657 | 26.828 | 27.941 | 28.770 | 28.343 |
| 24.485 | 27.113 | 30.000 | 29.172 | 29.598 |
| 25.314 | 27.657 | 30.828 | 33.598 | 33.172 |
| 26.142 | 28.485 | 31.657 | 34.000 | 34.426 |
| 26.284 | 29.314 | 32.485 | 34.828 | 38.000 |
| 26.971 | 30.142 | 32.770 | 35.657 | 38.828 |
| 27.799 | 30.971 | 33.314 | 36.485 | 39.255 |
| 28.627 | 31.799 | 34.142 | 37.314 | 39.657 |
| 29.456 | 31.941 | 34.971 | 38.142 | 40.485 |
| 30.284 | 32.627 | 35.799 | 38.426 | 41.314 |
| 31.113 | 33.456 | 36.627 | 38.971 | 42.142 |
| 0.000 | 34.284 | 37.456 | 39.799 | 42.971 |
| 0.000 | 35.113 | 37.598 | 40.627 | 43.799 |
| 0.000 | 35.941 | 38.284 | 41.456 | 44.083 |
| 0.000 | 36.770 | 39.113 | 42.284 | 44.627 |
| 0.000 | 0.000 | 39.941 | 43.113 | 45.456 |
| 0.000 | 0.000 | 40.770 | 43.255 | 46.284 |
| 0.000 | 0.000 | 41.598 | 43.941 | 47.113 |
| 0.000 | 0.000 | 42.426 | 44.770 | 47.941 |
| 0.000 | 0.000 | 0.000 | 45.598 | 48.770 |
| 0.000 | 0.000 | 0.000 | 46.426 | 48.912 |
| 0.000 | 0.000 | 0.000 | 47.255 | 49.598 |
| 0.000 | 0.000 | 0.000 | 48.083 | 50.426 |
| 0.000 | 0.000 | 0.000 | 0.000 | 51.255 |
| 0.000 | 0.000 | 0.000 | 0.000 | 52.083 |
| 0.000 | 0.000 | 0.000 | 0.000 | 52.912 |
| 0.000 | 0.000 | 0.000 | 0.000 | 53.740 |

FIG. A2 - Odd intermodulation product frequencies by order

| | | | | |
|---|---|---|---|---|
| 0.201 | 0.343 | 0.485 | 0.627 | 1.029 |
| 1.172 | 1.314 | 1.858 | 2.000 | 2.142 |
| 2.686 | 2.828 | 2.971 | 3.515 | 3.657 |
| 3.799 | 4.201 | 4.343 | 4.485 | 4.627 |
| 5.029 | 5.172 | 5.314 | 5.456 | 5.858 |
| 6.000 | 6.142 | 6.686 | 6.828 | 6.971 |
| 7.515 | 7.657 | 7.799 | 8.343 | 8.485 |
| 8.627 | 9.029 | 9.172 | 9.314 | 9.456 |
| 9.858 | 10.000 | 10.142 | 10.284 | 10.686 |
| 10.828 | 10.971 | 11.515 | 11.657 | 11.799 |
| 12.343 | 12.485 | 12.627 | 13.172 | 13.314 |
| 13.456 | 13.858 | 14.000 | 14.142 | 14.284 |
| 14.686 | 14.828 | 14.971 | 15.113 | 15.515 |
| 15.657 | 15.799 | 16.343 | 16.485 | 16.627 |
| 17.172 | 17.314 | 17.456 | 18.000 | 18.142 |
| 18.284 | 18.686 | 18.828 | 18.971 | 19.113 |
| 19.515 | 19.657 | 19.799 | 19.941 | 20.343 |
| 20.485 | 20.627 | 21.172 | 21.314 | 21.456 |
| 22.000 | 22.142 | 22.284 | 22.828 | 22.971 |
| 23.113 | 23.515 | 23.657 | 23.799 | 23.941 |
| 24.343 | 24.485 | 24.627 | 24.770 | 25.172 |
| 25.314 | 25.456 | 26.000 | 26.142 | 26.284 |
| 26.828 | 26.971 | 27.113 | 27.657 | 27.799 |
| 27.941 | 28.343 | 28.485 | 28.627 | 28.770 |
| 29.172 | 29.314 | 29.456 | 29.598 | 30.000 |
| 30.142 | 30.284 | 30.828 | 30.971 | 31.113 |
| 31.657 | 31.799 | 31.941 | 32.485 | 32.627 |
| 32.770 | 33.172 | 33.314 | 33.456 | 33.598 |
| 34.000 | 34.142 | 34.284 | 34.426 | 34.828 |
| 34.971 | 35.113 | 35.657 | 35.799 | 35.941 |
| 36.485 | 36.627 | 36.770 | 37.314 | 37.456 |
| 37.598 | 38.000 | 38.142 | 38.284 | 38.426 |
| 38.828 | 38.971 | 39.113 | 39.255 | 39.657 |
| 39.799 | 39.941 | 40.485 | 40.627 | 40.770 |
| 41.314 | 41.456 | 41.598 | 42.142 | 42.284 |
| 42.426 | 42.971 | 43.113 | 43.255 | 43.799 |
| 43.941 | 44.083 | 44.627 | 44.770 | 45.456 |
| 45.598 | 46.284 | 46.426 | 47.113 | 47.255 |
| 47.941 | 48.083 | 48.770 | 48.912 | 49.598 |
| 50.426 | 51.255 | 52.083 | 52.912 | 53.740 |

FIG. A3 - Sum of intermodulation products up to order 19